Article

Geochemical Investigation of Tar Balls Collected in a Brazilian Beach Using Biomarkers, Ni/V, δ¹³C Ratios and Ultra-High Resolution FT-ICR Mass Spectrometry

Bárbara D. Lima,[a] Laercio L. Martins,[a] Lívia C. Santos,[a] Eliane S. de Souza,[a] Marcos A. Pudenzi,[b] Heliara L. Nascimento,[b] Marcos N. Eberlin[b] and Georgiana F. da Cruz ⦿ *,[a]*

[a]*Laboratório de Engenharia e Exploração de Petróleo (LENEP), Universidade Estadual do Norte Fluminense Darcy Ribeiro (UENF), 27910-970 Macaé-RJ, Brazil*

[b]*Instituto de Química, Universidade Estadual de Campinas (Unicamp), CP 6154, 13083-970 Campinas-SP, Brazil*

Representative tar balls collected in two distinct years (2012 and 2014) in a beach along the State of Bahia, northeastern Brazil, were geochemically characterized in order to identify correlations between them and investigate potential sources. Terpanes and steranes biomarkers (detected by gas chromatography coupled to mass spectrometry, GC-MS), carbon stable isotope ratio (δ¹³C), Ni and V ratios and polar compounds by Fourier transform ion cyclotron resonance mass spectrometry using electrospray ionization in negative mode (ESI(–) FT-ICR MS) were evaluated. Three Brazilian oil samples from distinct sources were assessed as possible spill sources, comparing their results with the tar ball samples. Using chemometric techniques, it was verified correlation between the two set of tar ball samples, suggesting same source. However, no correlation with the oil samples was observed, with different geochemical profile among them. The heteroatom class distribution displayed severe degradation levels for tar balls and its seems that photo-oxidation and biodegradation processes were further relevant. Tar ball samples show multiple classes, most oxygenated, and with one sample showing considerable relative abundance of N_1 class, suggesting it is from a more recent oil spill. In brief, our results suggest that the region, with very sensitive ecosystem, is possibly subjected to frequent spills from the same source.

Keywords: oil spill, tar ball, weathering process, geochemical analysis, FT-ICR MS

Introduction

An examination of reports from several sources, including industry, government and academic, indicates that, although the diversified sources of petroleum input to the sea, they can be arranged into four main groups: petroleum transportation, natural seeps, petroleum production and petroleum consumption.[1] Among such groups, petroleum transportation is a potential spill source as a result of its activity that involves continuous flow of oil fields to final consumption.[2]

Most of the Brazilian oil exploration, exploitation, refining, and oil transporting activities are concentrated in coastal areas including northeastern coast,[3] region where tar ball samples investigated in this work were collected.

Some of these activities increase the risk of oil spills related to accidents due to collisions or groundings, accidental or deliberate releases of bilge and ballast water from ships,[4,5] justifying the tar balls appearing on the coast. Despite its intensity and importance, very few studies related to oil spill along Brazilian coast have been conducted.[6]

The oil spills frequently arriving to the northeastern Brazilian beaches are conducted by the South Atlantic subtropical current and by the wind-driven circulation of the South Atlantic Ocean that provides, near the surface, the large anticyclonic gyre of midlatitudes (15-30° S).[7] These oil spill events can bring irreversible and tragic environmental impacts to this region, which contains the greatest area of coral reefs along the entire Brazilian coast.[8]

With aging, the spilled oil eventually forms tar balls, which are soft clumps of weathered oil mixed with sand or other materials by wave action, normally found along

*e-mail: georgiana@lenep.uenf.br
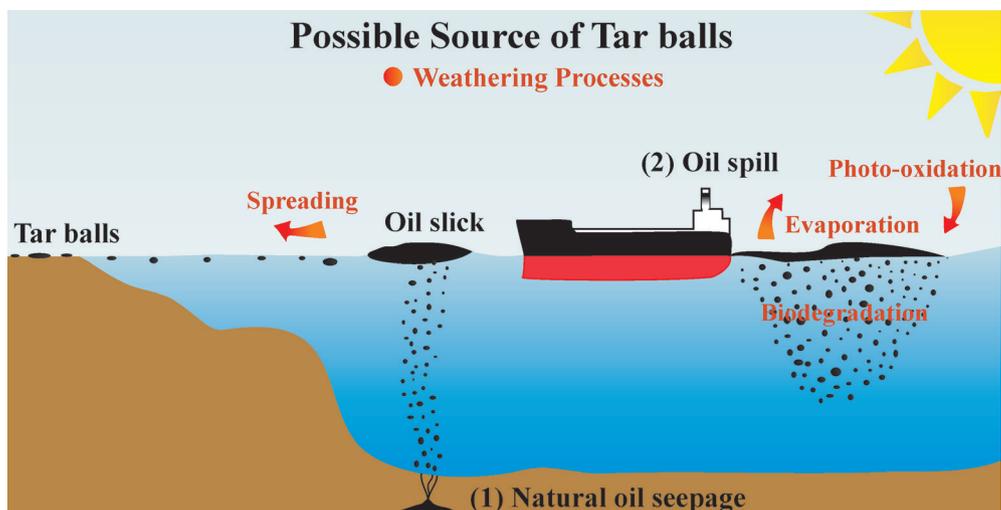
Figure 1. Possible source of the tar balls: natural oil seepage (1); oil spill (2). In addition to some weathering processes undergone by the oil slick at the sea: photo-oxidation; evaporation; biodegradation; and spreading (adapted from ITOPF[9] and Bourgault *et al.*).[10]

coastlines in oil producing areas, as showed in Figure 1. Once spilled on water, the oil undergoes several physical and chemical changes, not all at the same rate, but all starting as soon as oil is released, that alter its chemical composition. Those changes are collectively termed weathering (Figure 1).[1,11]

At the earliest stage after an oil spill, evaporation normally causes considerable weight loss of light hydrocarbons. Photo-oxidation then depletes certain aromatic hydrocarbons, including methyl-phenanthrene and methyl-chrysene.[12] Oil weathering can also increase the levels of oxygenated constituents, mainly by photo-oxidation and biodegradation processes, and deplete saturates and aromatic hydrocarbons.[13] When the task is to identify the source of the oils spill, these drastic changes in chemical composition of the spilled oil, which also affects oil's toxicity and hence it is biological impact add great difficulties. Geochemists and analytical chemists are therefore always searching for more efficient and unambiguous approaches to trace spilled oils of different natures, forms and types.[14]

Geochemical analysis of source-characteristic using environmentally-persistent petroleum biomarkers (Figure 2) such as terpanes, steranes, polycyclic aromatics and more recently, polar components, have uncovered crucial information in determining the source of spilled oil. It also helps to monitor the degradation process and to determine the weathering state of oils under a broad variety of conditions. Biomarker fingerprinting of spilled oils done by gas chromatography coupled to mass spectrometry (GC-MS) analysis has been the preferred technique applied to almost all oil spill investigations,[14-20] although no single parameter has been proved to provide unambiguous tracing. Individual biomarker parameters are only valuable and meaningful when assessed together with other parameters.[21]
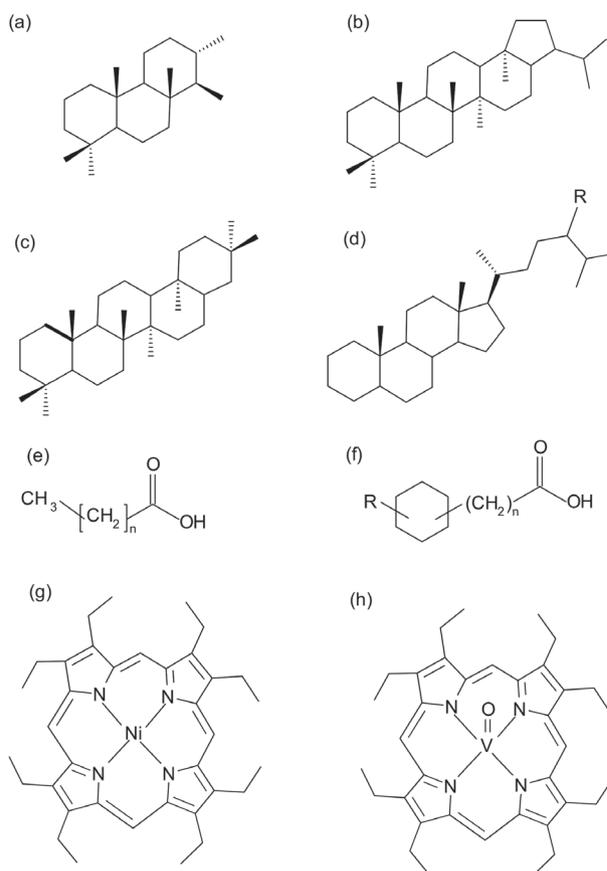
Figure 2. Representative molecular structure of key compounds presented in petroleum composition, and used herein to investigate tar ball samples. (a) Tricyclic terpane; (b) pentacyclic terpane (hopane); (c) non hopane petancyclic terpane (gammacerane); (d) sterane; (e) acyclic and (f) cyclic naphthenic acids; (g) nickel and (h) vanadium porphyrins.

Similar to other classic oil biomarkers, petroporphyrins (porphyrin compounds chelated with metals, such as vanadium and nickel, Figure 2) break down very slowly in the environment,[14,21] hence Ni/V ratios have been used

to trace spilled oils.[22,23] Together with Ni/V ratio, results of $\delta^{13}C$ ratio of whole oil or specific and individual compound such as *n*-alkanes have been used as biomarker diagnostic ratio to determine genetic relationships among oils and bitumes.[24] The $\delta^{13}C$ signatures has been shown to work efficiently in correlating spilled oils, even for samples subjected to severe weathering.[25-28]

More recently, the MS-petroleomics approach, via which thousands of polar crude oil constituents are identified via ultrahigh-resolution,[29] can be also applied to tar balls characterization. Fourier transform ion cyclotron resonance mass spectrometry (FT-ICR MS) has proved to be very useful to characterize spilled oils determining the degree of weathering and estimating the spill time at the sea, especially because it detects mainly the environmentally persistent polar compounds.[30-32]

In this present study weathered tar balls samples collected in two different years (2012 and 2014) at a beach located in the northeastern region of Brazil were comprehensively characterized to search for spatial and temporal correlations between the tar ball samples set. Moreover, it was evaluated the correlation of this tar balls and three possible Brazilian oil spill sources. These sources were chosen since they were produced and/or transported by ships near the region where tar balls were found. The geochemical characterization was based on a measure of several parameters including saturated biomarkers ratios, $\delta^{13}C$ signature, Ni/V ratio and relative abundance of polar classes obtained by ESI(–) FT-ICR MS petroleomics analysis. Biomarker ratios, $\delta^{13}C$ and Ni/V ratio were evaluated using principal component analysis (PCA) in order to identify the relationship between characteristics extracted from the data.

Experimental

Samples, extraction and fractionation

Tar ball samples (Figure 3) were collected along 3 km on a beach in the northeastern of Brazil (13°54'13'' South; 38°56'09'' West), at two different times, January 2012 and 2014, using latex gloves, wrapped in aluminium foil and stored frozen. All samples were solid, impregnated with sand and with a characteristic odor of oil. Approximately 10 g of the tar ball samples were ground and pulverized for Soxhlet extraction with 80 mL of dichloromethane (DCM) as solvent, for a period of 12 h. An aliquot of 0.04 g of the extracted oil was separated into saturates, aromatics and polars fractions by liquid chromatography using activated silica gel-alumina column. Saturated hydrocarbon fraction was eluted with *n*-hexane, aromatic hydrocarbons with *n*-hexane:DCM (4:1) and polar with DCM:methanol (9:1)

(25 mL of each). All solvents were chromatographic grade (Sigma-Aldrich Chemical Co., St. Louis, USA). For the geochemical characterization analysis were selected 7 tar ball samples, four collected in 2012 (TB 8, TB 10, TB 11 and TB 28) and three collected in 2014 (TB (a), TB (b) and TB (c)), with more than 10% (m/m) of saturated fraction, which represent the most preserved samples. Three potential Brazilian oil spill sources (Oil 1, Oil 2 and Oil 3) were prepared in the same way.

Only the saturated fraction was considered for GC-MS analysis. The whole oil extract was used for stable carbon isotope analysis, nickel and vanadium ratio and petroleomic analysis by FT-ICR MS.

Figure 3. Tar ball samples collected on a beach in the northeastern of Brazil.

Saturated biomarkers

The saturated hydrocarbons (0.02 mg μL^{-1}) were analyzed with an Agilent 6890N gas chromatograph interfaced with an Agilent 5973-MSD mass-selective. Helium was used as the carrier gas at a constant flow rate at 1.0 mL min^{-1}. Sample extracts were injected in a splitless mode onto a 30 m × 0.25 mm (0.25 μm film thickness) DB-5MS fused capillary column at an initial temperature of 60 °C for 2 min. The temperature was programmed at 22 °C min^{-1} to 200 °C, held for 3 min, and heated up to 300 °C at a rate of 3 °C min^{-1} held at the final for 25 min. The injector and transfer line temperature was 300 and 280 °C, respectively. The mass spectrometer was operated at an electron energy of 70 eV with an ion source temperature of 230 °C. The MS was operated in a full scan (50 a 550 Da) and selected ion monitoring (SIM) mode and compound identifications were made by comparison with published reference spectra. Biomarker ratios that provide information of source and maturity were calculated using peak areas from SIM GC-MS chromatograms of *m/z* 191 for terpanes, *m/z* 217 for diasteranes and *m/z* 259 for tetracyclic polyprenoids.

Nickel/vanadium ratio

About 0.1 g of whole oil extracted for each tar ball and source samples were dissolved in HNO_3/H_2O_2 (3:2 v/v) and heated by microwave for 20 min at 170 ºC. The volume was completed to 15 mL with ultrapure water and the determination of nickel and vanadium was made in triplicate by inductively coupled plasma-optical emission spectrometry (720 series ICP OES, Agilent Technologies). The analysis conditions were: plasma power 1100 W, plasma gas flow 15.0 L min^{-1}, auxiliary gas flow 1.5 L min^{-1}, nebulizer gas flow 0.75 L min^{-1}, nebulizer SeaSpray with SinglePass chamber. Detection limits were 7.9 and 0.2 µg g^{-1} for Ni and V, respectively, and ratio were calculated using Ni and V content *per* sample.

$\delta^{13}C$ ratio

The $\delta^{13}C$ measurements in the tar ball and source samples were performed in triplicate (standard deviation better than 0.2‰) using 0.1 mg of the whole oil (unfractionated) directly for combustion in tin capsules in a mass spectrometer coupled to a gas chromatograph (ANCA-GSL Sercon Hidra 20-20). The results were expressed in the δ notation in parts *per* thousand (‰) relative to the international standard PDB (Cretaceous carbonate fossil *Bellemnitella americana* from PeeDee Formation in South Carolina, USA) for $^{13}C/^{12}C$ ratio.

Petroleomic by ESI(–) FT-ICR MS

Petroleomic analyze was performed by a Fourier transform ion cyclotron resonance mass spectrometry (FT-ICR MS 7.2T LTQ FT Ultra, ThermoScientific, Bremen, Germany) with resolving power of 400,000 on 200-1000 Da mass range. The methodology was the same used for polar fraction analysis of 30 Brazilian oils described by Martins *et al.*[33] The whole oil (2.0 mg) extracted from the tar ball and source samples were previously dissolved in 1.0 mL of toluene and then diluted with 1.0 mL of methanol, containing 0.2% of ammonium hydroxide. All solvents were of high performance liquid chromatography (HPLC) grade (Sigma-Aldrich Chemical Co., St. Louis, USA). Solutions of each sample were infused directly into negative ion mode electrospray ionization (ESI(–)) using a 5 µL min^{-1} syringe flow, with spray voltage of 3.1 kV. A 100 scans spectrum was acquired for each tar ball and source samples and the data were processed using PetroMS software.[34]

Chemometric analysis

The chemometric analysis were performed using the software Statistic 7.0.[35] Biomarker ratios, $\delta^{13}C$ signatures and Ni/V ratios data were explored by principal component analysis (PCA) on autoscaled columns data.

Results and Discussion

Geochemical approach: biomarkers, Ni/V and $\delta^{13}C$ ratios

Biomarkers are widely used in geochemical studies since they are normally resistant to microbial alteration and weathering, being also frequently used in oil spill investigations for petroleum contaminated environmental complex samples, such as tar balls.[26,36-39] Fingerprinting of terpane, sterane and other resistant biomarkers provides therefore a powerful tool to investigate the source, correlation and differentiation of weathered oils once their diagnostic ratios practically are not affected by weathering.[14,40] In this context, a series of key geochemical parameters were calculated based on the biomarkers family of terpanes (*m/z* 191 chromatogram), diasteranes (*m/z* 217 chromatogram) and tetracyclic poliporenoid (*m/z* 259 chromatogram), as presented in Table 1. Figure 4 shows the *m/z* 191 chromatograms, which contains most of compounds evaluated to oil samples Oil 1, Oil 2 and Oil 3, and two representative tar ball samples, TB 8 and TB (a), collected in 2012 and 2014, respectively.

It can be already observed in Figure 4 a similar profile in the mass chromatograms to the two tar ball samples, however being significantly different from the three oil samples. These results could be also observed in Table 1 to all tar ball samples, with similar parameters to them, being distinct to the oil samples. Note that the crude oils also present distinct biomarker profiles among them, since they are not from the same oil field.

In addition to the diagnostic biomarker ratios, Ni/(Ni + V) and $\delta^{13}C$ isotope ratio were used herein to investigate the tar ball samples, in correlation with the oil samples (results also presented in Table 1). Ni/(Ni + V) ratio is normally a reliable parameter since there is a direct correlation of such ratios with geosphere biomarkers and their corresponding biological precursors.[21] Besides, even under severe weathering, the corresponding metallo-porphyrins get lost in similar extents.[41] $\delta^{13}C$ signatures in oils also serves to track oil spills, since this ratio is inherited from the source organic matter, although it is influenced by the maturity and by physical and chemical alterations after generation.[22]

Table 1. Diagnostic ratios from saturated biomarkers compounds, nickel/vanadium and carbon stable isotope for spill sources (Oil 1, Oil 2 e Oil 3) and tar ball samples TB 8, TB 10, TB11 and TB 28 collected in 2012 and TB (a), TB (b) and TB (c) collected in 2014

Diagnostic ratios	Sample									
	Oil 1	Oil 2	Oil 3	TB 8	TB 10	TB 11	TB 28	TB (a)	TB (b)	TB (c)
Tr23/H30hop	0.65	2.68	0.26	1.68	1.59	1.69	1.49	1.34	1.59	1.26
H29/H30hop	0.57	0.60	0.82	0.82	0.83	0.81	0.89	1.03	0.84	1.05
Tr23/Tr24	1.12	1.39	1.42	2.68	2.54	2.54	2.26	2.42	2.53	2.08
Ts/(Ts + Tm)	0.43	0.84	0.24	0.41	0.43	0.43	0.44	0.27	0.44	0.55
Gam/H30hop	0.24	0.26	0.10	0.34	0.32	0.32	0.41	0.27	0.37	0.66
Tr21/Tr23	0.84	0.62	0.73	0.66	0.64	0.64	0.35	0.66	0.62	0.52
Tr20/Tr23	0.52	0.27	0.40	0.30	0.28	0.27	0.07	0.38	0.29	0.39
TPP/(TPP + Dia 27)	0.88	0.72	0.84	0.69	0.70	0.68	0.73	0.73	0.70	0.83
Ni/(Ni + V)	0.96	0.94	0.34	0.47	0.48	0.49	0.47	0.45	0.59	0.22
$\delta^{13}C$	−31.23	−28.00	−25.10	−24.03	−24.67	−24.13	−24.61	−23.99	−24.42	−27.63

Tr23/H30hop: tricyclic terpane C23 peak area over 17α(H),21β(H)-hopane peak area in *m/z* 191 chromatogram; H2/H30 hop: 17α(H),21β(H)-30-norhopane peak area over 17α(H),21β(H)-hopane peak area in *m/z* 191 chromatogram; Tr23/Tr24: tricyclic terpane C23 peak area over tricyclic terpane C24 peak area in *m/z* 191 chromatogram; Ts/(Ts + Tm): 18α(H)-22,29,30-trisnorneohopane peak area over 17α(H)-22,29,30-trisnorhopane peak area in *m/z* 191 chromatogram; Gam/C30 αβ: gammacerane peak area over 17α(H),21β(H)-hopane peak area in *m/z* 191 chromatogram; Tr21/Tr23: tricyclic terpane C21 peak area over tricyclic terpane C23 peak area in *m/z* 191 chromatogram; Tr20/Tr23: tricyclic terpane C20 peak area over tricyclic terpane C23 peak area in *m/z* 191 chromatogram; TPP/(TPP + Dia 27): tetracyclic poliprenoid peak area in *m/z* 259 over 13β(H),17α(H)-diacolestanes *S* and *R* peaks area in *m/z* 217 chromatogram.

To statistically evaluate the correlation between tar ball samples and the three possible spill sources, the results on Table 1 was investigated by principal component analysis (PCA). Figure 5 presents the results from the PCA to the source parameters. The PCA scores explain 73.43% of the model (sum of the principal components 1 and 2, which are 44.73 and 28.07%, respectively).

The seven tar ball samples were grouped in the 3rd and 4th quadrants (Figure 5a), being $\delta^{13}C$ and the ratios H29/H30hop, Tr23/Tr24 and Gam/H30hop the main factors responsible for this grouping. These diagnostic ratios show great weathering resistance and so have been used in several studies to characterize oil spills, their levels of degradation and their sources.[42-47] The great similarity on terpanes composition and $\delta^{13}C$ observed for tar ball samples can suggest that they are probably originated from the same spill source.

The Ni/(Ni + V) ratio is also an important parameter with similar contribution to PC1 and PC2, as observed in the loadings plot (Figure 5b) and suggests that all tar balls samples presents low and similar values of this parameter. This result also supports the same source hypothesis to tar balls. Previous study shows its ratio Ni to V did not change much after a long-term weathering.[48]

Based on the high values for TPP/(TPP + Dia 27) ratio, it is possible to suggest that oil spill samples and tar balls are derived from a low salinity environmental, once high concentrations of tetracyclic polyprenoid compounds (TPP)

are related to input non-marine algae organic matter.[49,50] This fact is reinforced by the low values of Gam/H30 hop ratio, since the presence of high concentrations of gammacerane results from hypersalinity environmental.[51]

However, the lack of correlation between the tar ball samples and the possible spill sources can be verified by their position in the scores plot (Figure 5a), as the position of samples Oil 1, Oil 2 and Oil 3 (quadrants 1 and 2, respectively): the three originated from different sedimentary basins. Due to this, none of possible source analyzed can be the tar balls source, once Oil 1, Oil 2 and Oil 3 show a completely different quadrant position. This way, the tar balls spill source can be from another petroleum production area, a natural seep and ship activities which should be investigating.

In order to extent the molecular analysis of the tar balls chemical composition to heteroatom polar compounds, and provide more comprehensively assessment of the weathered processes undergone by them, profiles of their acidic polar composition were obtained by ESI(−) FT-ICR MS analysis.

Petroleomics approach: polar compounds distribution

Assuming that the tar ball samples are from the same source, as supported by the results from geochemical parameters, the heteroatom class distribution was assessed in order to evaluate possible alterations caused by weathering processes, such as photo-oxidation and biodegradation.
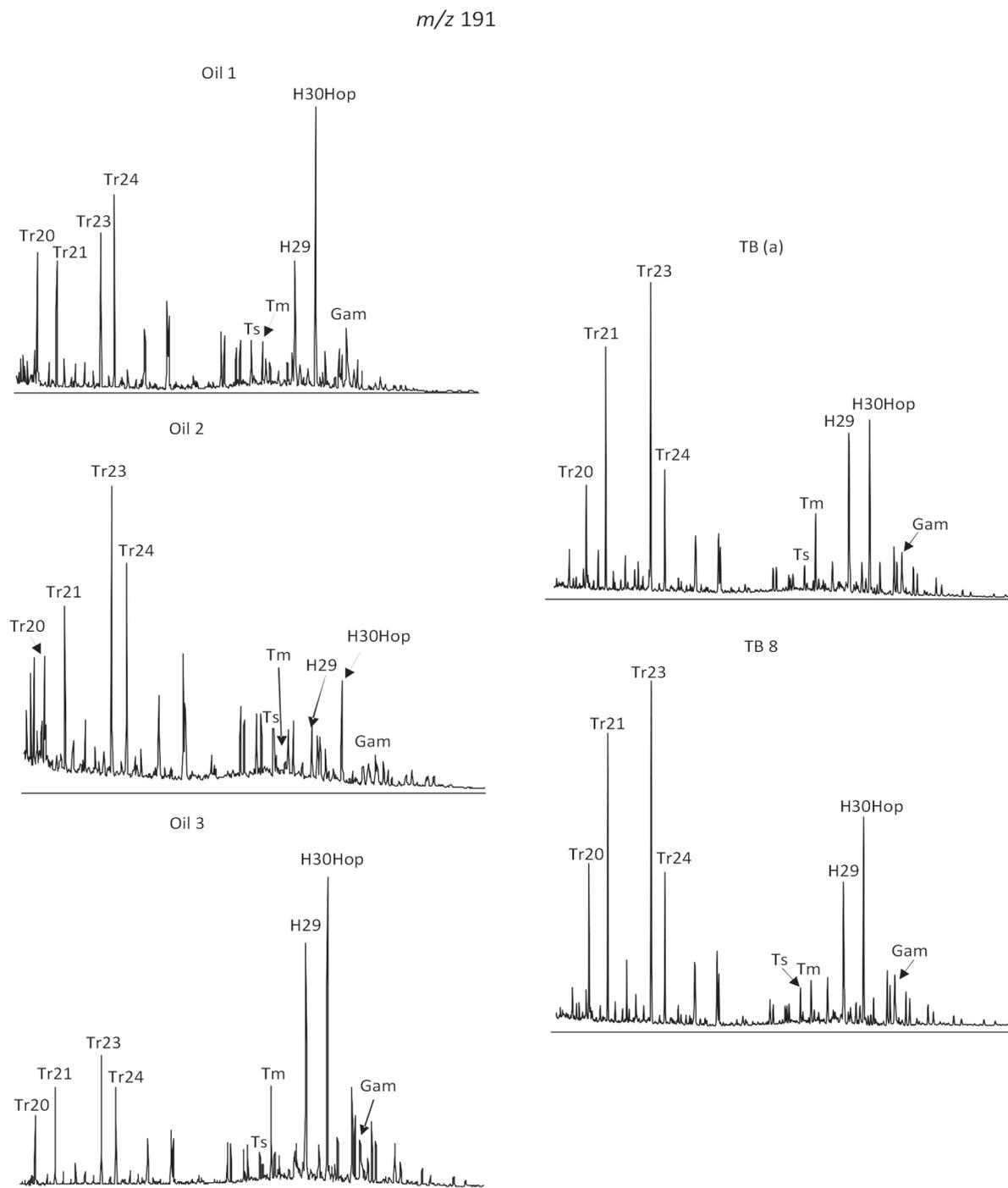
m/z 191

Figure 4. Mass chromatogram m/z 191 of saturated fraction of oil samples Oil 1, Oil 2 and Oil 3 and to representative samples of tar balls, TB 8 and TB (a), collected in 2012 and 2014, respectively. Where Tr20, Tr 21, Tr23 and Tr24: tricyclic terpane C20, C21, C23 and C24; Ts: 18α(H)-22,29,30-trisnorneohopane; Tm: 17α(H)-22,29,30-trisnorhopane; H29: 17α(H),21β(H)-30-norhopane; H30Hop: 17α(H),21β(H)-hopane; Gam: gammacerane.

Figure 6 shows the relative abundance of polar heteroatom classes obtained by the ESI(–) FT-ICR MS analysis for all tar ball samples, that comprise acidic compounds which are able to deprotonate such as carboxylic acids, alcohols and pyrroles.[52,53] The most abundant were oxygen-containing classes, mainly O_2, O_3 and O_4 classes, whereas sulfur-containing classes were detected in lower abundance,

with the O_xS classes presenting greater percentage, such as O_3S and O_4S. Nitrogen-containing classes presented intermediate abundance, also with the oxygenated ones (N_1O_x showing higher percentage).

It can be observed in Figure 6 that tar ball samples collected in 2012 present more similar polar composition, that is also more similar to sample TB (b) collected in
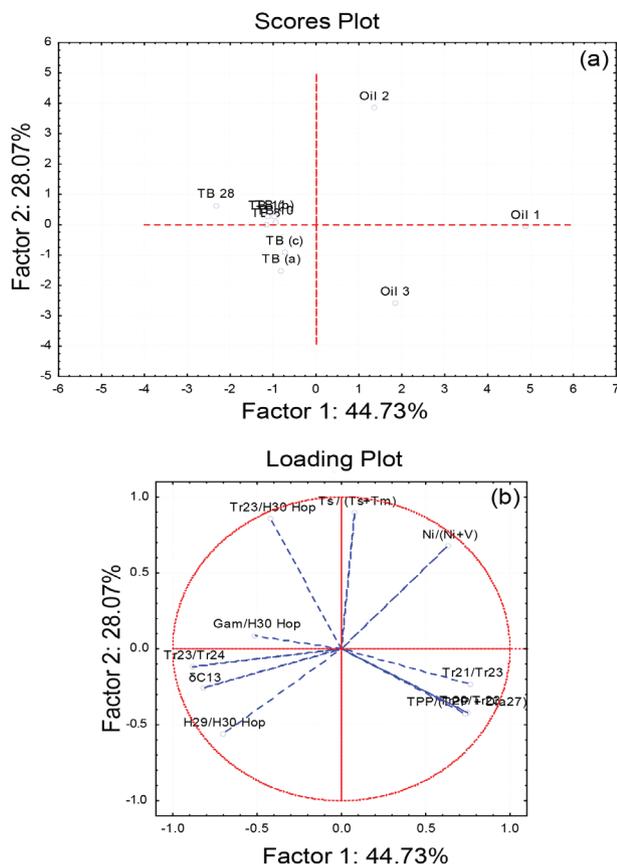
Figure 5. Scores (a) and loadings (b) plot for principal components analysis of the Ni/(Ni + V), $\delta^{13}C$ and diagnostic ratios from saturated biomarkers compounds for tar ball samples (TB 8, TB, 10, TB 11, TB 28, TB (a), TB (b) and TB (c)) and spill source (Oil 1, Oil 2 and Oil 3).

2014. On the other hand, samples collected in 2014 present significantly distinct heteroatom class distribution, which should indicate different intensity of the weathered processes. Highest relative abundance of O_3 and O_4 classes is not common in produced crude oils, and is normally an indication of the photo-oxidation processes undergone by weathered oil spills.[31,54] Its suggested that oxidation proceeds in series, and that once oxidized, compounds are more susceptible to further oxidation.[54] Based on that, tar ball sample TB (c) seems the most photo-oxidized one, presenting also O_5 and O_6 polar compounds in its composition.

It is worthy to mention that the unique sample presenting N_1 class in the polar composition is the tar ball TB (a) (Figure 6), with highest relative abundance among the nitrogen classes (18%). Since the N_1 class is known to decrease in relative abundance with increasing weathering extent, whereas O-containing classes such as NO and O_x increase,[32] Figure 6 suggests that all tar balls except sample TB (a) have been extensively weathered. Weathered products are known to be formed, mainly by photo-oxidation,[54] which generates mostly oxygen products.
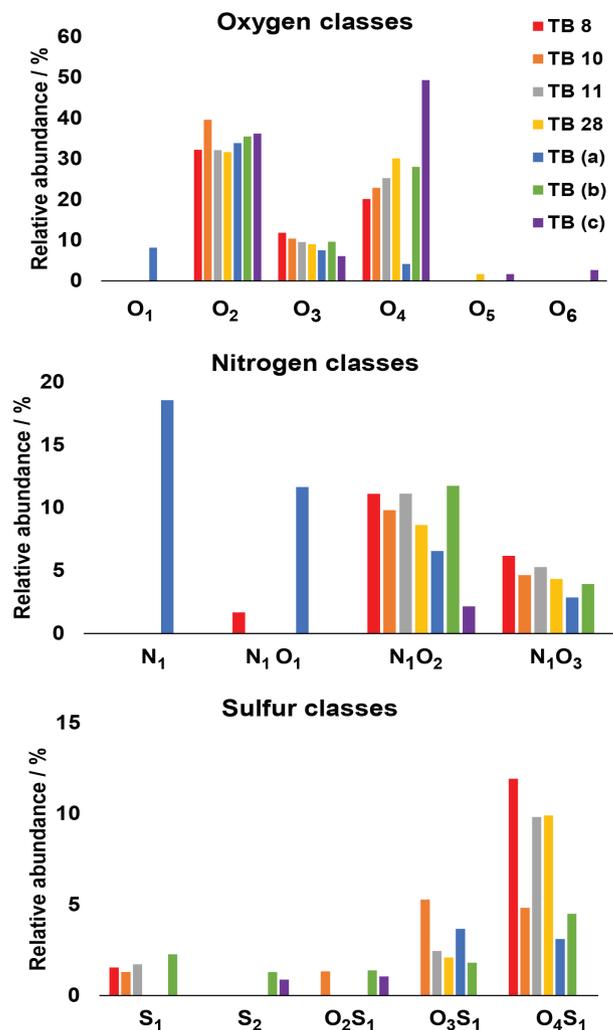
Figure 6. Heteroatom class distributions for four tar balls samples TB 8, TB 10, TB 11 and TB 28, collected in 2012 and three tar ball samples TB (a), TB (b) and TB (c), collected in 2014.

Previous study have been observed that the N_1 class was persistent until 511 days after spill and have a severe decrease after 617 days.[32] In this way considering that all tar balls came from the same oil spilled source, sample TB (a) seems indeed to have been subjected to much less weathering extent. The exclusive detection of the O_1 class, the highest relative abundance to N_1O_1 class and its lowest abundance for the O_4 class, which are formed by products of weathering, corroborate this hypothesis. This fact may be related to a more recent event for TB (a) compared to other tar balls, which suggests that the region of the Brazilian coast where the tar balls were found is target of periodic spillage from the same source.

Even if the spilled oil was already a biodegraded oil before it was released in the environment, it probably could not had high abundance of the O_3 and O_4 classes, which contain weathered products mainly formed by photo-oxidation, and not biodegradation.[55] Thereby, the

presence of high abundance of O_2 class and low abundance of O_3 and O_4 classes for sample TB (a) can indicate that this samples was already a biodegraded oil before the spill, since biodegradation leads to the predominantly increases of O_2 class, attributed to the formation of naphtenic acids via oxidation of hydrocarbons.[33,56] These results are also in agreement with other study,[30] which detected oxygenated species, mainly O_3 and O_4 classes, in high abundance in an oil extracted from crude oil contaminated soil, collected in Long Beach, Los Angeles County, California.

To assess the possibility of biodegradation as one prominent process during of the weathering of the tar balls, some biodegradation indexes suggested in a previous works based on distribution of O_2 class were applied: modified A/C ratio[57] and modified SA index[33] (Figure 7). The modified A/C ratio is calculated by the relative abundance of acyclic acids (DBE 1) over the cyclic acids (DBE 2 to 6), while modified SA index is calculated by the sum of the relative abundance of DBE 2-6 for O_2 class.
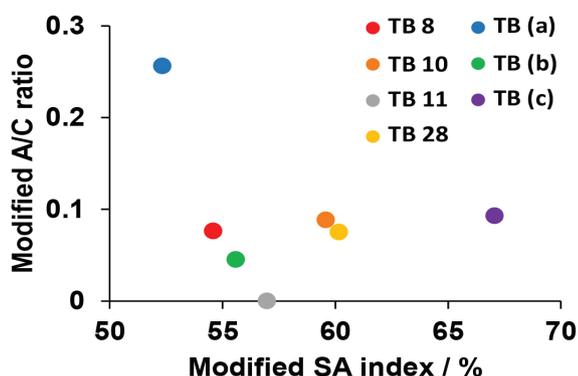
Figure 7. Comparison of biodegradation evaluation parameters for tar ball samples TB 8, TB 10, TB 11 and TB 28, collected in 2012 and tar ball samples TB (a), TB (b) and TB (c), collected in 2014.

Modified A/C ratio tends to decrease while modified SA index tends to increase with biodegradation. The tar ball samples present modified A/C ratio lower than 0.1, excepted to sample TB (a), which normally indicate heavy to very severe level of biodegradation to crude oils.[33,56]

Besides, considering that the tar ball TB (a) was provide from a more recent spill, the trend form all tar ball samples would be similar to it if biodegradation were not expressive. However, Figure 7 shows different behavior in general, which suggest biodegradation was a relevant process undergone by the oil spilled probably while still in the sea water, leading to the heteroatomic compositional modification. These indexes also suggest that sample TB (c) has higher biodegradation level, besides to show higher O_4 content and some O_5 and O_6 content (Figure 6), which characterize photo-oxidation, implying that was exposed to more extensive weathering.

Conclusions

The comprehensive analysis of seven tar balls collected at the same area in a northeastern Brazilian beach but at different times with two years interval (2012 and 2014) indicated that these samples have the same spill origin. Regarding the possible sources, PCA analyzes for the diagnostic ratios from saturated biomarkers, mainly H29/H30hop, Tr23/Tr24, Gam/H30hop, and TPP ratios, as well as $\delta^{13}C$ and Ni/V ratio showed that the potential Oil 1, Oil 2 and Oil 3 samples can not be considered as the spill source of the evaluated tar balls.

In addition, the heteroatom class profiles obtained by FT-ICR MS pointed out extensive weathering for all samples, with biodegradation and photo-oxidation as the most important processes undergone by the crude oil that originated the tar ball samples while in the sea water. Sample TB (a) was less degraded, suggesting that this sample was from the same oil source but generated from a more recent oil spill.

In summary, the comprehensive chemical analysis presented herein supports the hypothesis that the Brazilian Northeastern coast is frequently target of same spills, originated from natural seepage or anthropogenic activities as transportation and exploration, since no serious spill accidents in the South Atlantic Ocean have been reported in the area. Indeed, scrutinizing the chemical composition of tar balls functions as an important strategy to track oils spills and their chronology whereas revealing details of the chemical transformations occurring during oil weathering.

Acknowledgments

References

1. National Research Council; *Oil in the Sea III: Inputs, Fates and Effects*, 1st ed.; The National Academies Press: Washington, DC, 2003.

2. Rodrigue, J. P.; *Cah. Géogr. Qué.* **2004**, *48*, 357, DOI: 10.7202/011797ar.

3. Agência Nacional do Petróleo, Gás Natural e Biocombustíveis (ANP); *Anuário Estatístico Basileiro do Petróleo, Gás Natural*

e Biocombustíveis; Rio de Janeiro, 2018, available at http://www.anp.gov.br/publicacoes/anuario-estatistico/5237-anuario-estatistico-2019, accessed in September 2019.

4. Lucas, Z.; MacGregor, C.; *Mar. Pollut. Bull.* **2006**, *52*, 778.

5. Romero, A. F.; Abessa, D. M. S.; Fontes, R. F. C.; Silva, G. H.; *Mar. Pollut. Bull.* **2013**, *74*, 156.

6. Neto, J. B. A.; Campos, T. F. C.; Andrade, C. D. P.; Sichel, S. E.; Fonseca, E. M.; Motoki, A.; *Environ. Geochem. Health* **2014**, *36*, 1199.

7. Reid, J. L.; *Prog. Oceanogr.* **1986**, *56*, 137.

8. Leão, Z. M. A. N.; Dominguez, J. M. L.; *Mar. Pollut. Bull.* **2000**, *41*, 112.

9. International Tanker Owners Pollution Federation (ITOPF); *Fate of Marine Oil Spills, Technical Information Paper 2*; International Tanker Owners Pollution Federation Limited, 2011, available at https://www.itopf.org/knowledge-resources/documents-guides/document/tip-02-fate-of-marine-oil-spills/, accessed in September 2019.

10. Bourgault, D.; Tremblay, H.; Schloss, I. R.; Plante, S.; Archambault, P.; *Case Stud. Environ.* **2017**, DOI: 10.1525/cse.2017.sc.454841.

11. Yang, C.; Wang, Z.; Brown, C. E.; Landriault, M.; Yang, Z.; Hollebone, B.; Lambert, P.; Zhang, G. In *Oil Spill Environmental Forensics Case Studies*; Stout, S.; Wang, Z., eds.; Butterworth-Heinemann: Oxford, 2017, ch. 3.

12. Radovic, J. R.; Aeppli, C.; Nelson, R. K.; Jimenez, N.; Reddy, C. M.; Bayona, J. M.; Albaigés, J.; *Mar. Pollut. Bull.* **2014**, *79*, 268.

13. Aeppli, C.; Carmichael, C. A.; Nelson, R. K.; Lemkau, K. L.; Graham, W. M.; Redmond, M. C.; Valentine, D. L.; Reddy, C. M.; *Environ. Sci. Technol.* **2012**, *46*, 8799.

14. Wang, Z.; Fingas, M.; Page, D. S.; *J. Chromatogr. A* **1999**, *24*, 1537.

15. Volkman, J. K.; Holdsworth, D. G.; Neill, G. P.; Bavor, H. J.; *Sci. Total Environ.* **1992**, *112*, 203.

16. Munoz, D.; Guiliano, M.; Doumenq, P.; Jacquot, F.; Scherrer, P.; Mille, G.; *Mar. Pollut. Bull.* **1997**, *34*, 868.

17. Wang, Z.; Fingas, M.; Yang, C.; Hollebone, B.; *Prepr. - Am. Chem. Soc., Div. Energy Fuels* **2004**, *49*, 331.

18. Chandru, K.; Zakaria, M. P.; Anita, S.; Shahbazi, A.; Sakari, M.; Bahry, P. S.; Mohamed, C. A. R.; *Mar. Pollut. Bull.* **2008**, *56*, 950.

19. Wang, C.; Chen, B.; Zhang, B.; He, S.; Zhao, M.; *Mar. Pollut. Bull.* **2013**, *71*, 64.

20. Wang, C.; Chen, B.; Zhang, B.; Guo, P.; Zhao, M.; *Environ. Sci.: Processes Impacts* **2014**, *16*, 2408.

21. Wang, Z.; Yang, C.; Fingas, M.; Hollebone, B.; Yim, U. H.; Oh, J. R. In *Oil Spill Environmental Forensics*; Wang, Z.; Stout, S., eds.; Academic Press: London, 2007, ch. 3.

22. Jeffrey, A. W. A. In *Oil Spill Environmental Forensics*; Wang, Z.; Stout, S., eds.; Academic Press: London, 2007, ch. 6.

23. Lobão, M. M.; Cardoso, J. N.; Mello, M. R.; Brooks, P. W.; Lopes, C. C.; Lopes, R. S. C.; *Mar. Pollut. Bull.* **2010**, *60*, 2263.

24. Peters, K. E.; Walters, C. C.; Moldowan, J. M.; *The Biomarker Guide: Biomarkers and Isotopes in the Environment and Human History*, 2nd ed.; Cambridge University Press: Cambridge, 2005.

25. Lewan, M. D.; Warden, A.; Dias, R. F.; Lowry, Z. K.; Hannah, T. L.; Lillis, P. G.; Kokaly, R. F.; Hoefen, T. M.; Swayze, G. A.; Mills, C. T.; Harris, S. H.; Plumlee, G. S.; *Org. Geochem.* **2014**, *75*, 54.

26. Wang, Z.; Fingas, M.; Landriault, M.; Sigouin, L.; Castle, B.; Hostetter, D.; Zhang, D.; Spencer, B.; *J. High Resolut. Chromatogr.* **1998**, *21*, 383.

27. Suneel, V.; Vethamony, P.; Zakaria, M. P.; Naik, B. G.; Prasad, K. V. S. R.; *Mar. Pollut. Bull.* **2013**, *70*, 81.

28. Wang, M.; Wang, C.; He, S.; *Aquat. Procedia* **2015**, *3*, 197.

29. Marshall, A. G.; Rodgers, R. P.; *Proc. Natl. Acad. Sci. U. S. A.* **2008**, *105*, 18090.

30. Hughey, C. A.; Galasso, S. A.; Zumberge, J. E.; *Fuel* **2007**, *86*, 758.

31. Islam, A.; Cho, Y.; Yim, U. H.; Shim, W. J.; Kim, Y. H.; Kim, S.; *J. Hazard. Mater.* **2013**, *263*, 404.

32. Corilo, Y. E.; Podgorski, D. C.; Mckenna, A. M.; Lemkau, K. L.; Reddy, C. M.; Marshall, A. G.; Rodgers, R. P.; *Anal. Chem.* **2013**, *85*, 9064.

33. Martins, L. L.; Pudenzi, M. A.; Cruz, G. F.; Nascimento, H. D. L.; Eberlin, M, N.; *Energy Fuels* **2017**, *31*, 6649.

34. Corilo, Y. E.; Vaz, B. G.; Simas, R. C.; Nascimento, H. D. L.; Klitzke, C. F.; Pereira, R. C. L.; Bastos, W. L.; Neto, E. V. S.; Rodgers, P. R.; Eberlin, M. N.; *Anal. Chem.* **2010**, *82*, 3990.

35. *Statistica Software 7.0*, version 7.0.61.0; StatSoft, Tulsa, OK, USA, 2004.

36. Seifert, W. K.; Moldowan, J. M.; *Geochim. Cosmochim. Acta* **1979**, *43*, 111.

37. Wang, Z.; Fingas, M.; Owens, E. H.; Sigouin, L.; Brown, C. E.; *J. Chromatogr. A* **2001**, *926*, 275.

38. Mulabagal, V.; Yin, F.; John, G. F.; Hayworth, J. S.; Clement, T. P.; *Mar. Pollut. Bull.* **2013**, *70*, 147

39. Volkman, J. K.; Alexander, R.; Kagi, R. I.; Rowland, S. J.; Sheppard, P. N.; *Org. Geochem.* **1984**, *6*, 619.

40. Wang, Z.; Yang, C.; Yang, Z.; Brown, C. E.; Hollebone, B. P.; Stout, S. A. In *Standard Handbook Oil Spill Environmental Forensics*; Stout, S. A.; Wang, Z., eds.; Academic Press: Cambridge, 2016, ch. 4.

41. Lavilla, I.; Vilas, P.; Millos, J.; Bendicho, C.; *Anal. Chim. Acta* **2006**, *577*, 119.

42. Kvenvolden, K. A.; Hostettler, F. D.; Carlson, P. R.; Rapp, J. B.; *Environ. Sci. Technol.* **1995**, *29*, 2684.

43. Stout. S. A.; Uhler, A. D.; Mccarthy, K. J. A.; *Environ. Forensics* **2001**, *2*, 87.

44. Wang, Z.; Yang, C.; Yang, Z.; Sun, J.; Hollebone, B.; Brown, C.; Landriault, M.; *J. Environ. Monit.* **2011**, *13*, 3004.

45. Wang, Z.; Yang, C.; Fingas, M.; Hollebone, B.; Peng, X.; Hansen, A. B.; Christensen, J. H.; *Environ. Sci. Technol.* **2005**, *39*, 8700.

46. Wang, Z.; Stout, S. A.; Fingas, M.; *Environ. Forensics* **2006**, *7*, 105.

47. Little, D. I.; Galperin, Y.; Bullimore, B.; Camplin, M.; *Environ. Sci.: Processes Impacts* **2015**, *17*, 398.

48. Liu, X. In *Oil Spill Environmental Forensics Case Studies*; Stout, S.; Wang, Z., eds.; Butterworth-Heinemann: Oxford, 2017, ch. 11.

49. Holba, A. G.; Tegelaar, E.; Ellis, L.; Singletary, M. S.; Albrecht, P.; *Geology* **2000**, *28*, 251.

50. Holba, A. G.; Dzou, L. I.; Wood, G. D.; Ellis, L.; Adam, P.; Schaeffer, P.; Albrecht, P.; Greene, T.; Hughes, W. B.; *Org. Geochem.* **2003**, *34*, 441.

51. Mello, M. R.; Telnaes, N.; Gaglianone, P. C.; Chicarelli, M. I.; Brassell, S. C.; Maxwell, J. R.; *Org. Geochem.* **1988**, *13*, 31.

52. Qian, K.; Robbins, W. K.; Hughey, C. A.; Cooper, H. J.; Rodgers, R. P.; Marshall, A. G.; *Energy Fuels* **2001**, *15*, 1505.

53. Oldenburg, T. B. P.; Brown, M.; Bennett, B.; Larter, S. R.; *Org. Geochem.* **2014**, *75*, 151.

54. Ray, P. Z.; Chen, H.; Podgorski, D. C.; Mckenna, A. M.; Tarr, M. A.; *J. Hazard. Mater.* **2014**, *280*, 636.

55. King, S. M.; Leaf, P. A.; Olson, A. C.; Ray, P. Z.; Tarr, M. A.; *Chemosphere* **2014**, *95*, 415.

56. Kim, S.; Stanford, L. A.; Rodgers, R. P.; Marshall, A. G.; Walters, C. C.; Qian, K.; Wenger, L. M.; Mankiewicz, P.; *Org. Geochem.* **2005**, *36*, 1117.

57. Vaz, B. G.; Silva, R. C.; Klitzke, C. F.; Simas, R. C.; Nascimento, H. D. L.; Pereira, R. C. L.; Garcia, D. F.; Eberlin, M. N.; Azevedo, D. A.; *Energy Fuels* **2013**, *27*, 1277.